Mixing Models for Large-Eddy Simulation of Nonpremixed Turbulent Combustion

S. M. deBruynKops
Lecturer

J. J. Riley
Professor

Department of Mechanical Engineering,
University of Washington,
Box 352600,
Seattle, WA 98195-2600

The application of mixture fraction based models to large-eddy simulations (LES) of nonpremixed turbulent combustion requires information about mixing at length scales not resolved on the LES grid. For instance, the large-eddy laminar flamelet model (LELFM) takes the subgrid-scale variance and the filtered dissipation rate of the mixture fraction as inputs. Since chemical reaction rates in nonpremixed turbulence are largely governed by the mixing rate, accurate mixing models are required if mixture fraction methods are to be successfully used to predict species concentrations in large-eddy simulations. In this paper, several models for the SGS scalar variance and the filtered scalar dissipation rate are systematically evaluated a priori using benchmark data from a DNS in homogeneous, isotropic, isothermal turbulence. The mixing models are also evaluated a posteriori by applying them to actual LES data of the same flow. Predictions from the models that depend on an assumed form for the scalar energy spectrum are very good for the flow considered, and are better than those from models that rely on other assumptions.
[DOI: 10.1115/1.1366679]

1 Introduction

In large-eddy simulations of nonreacting flows, the models for the unresolved terms in the momentum and conserved scalar equations rely on the fact that most of the kinetic and scalar energy resides in the largest scales. It is sometimes reasoned that a subgrid model need only extract the correct amount of energy from the large scales to be adequate for many applications. The same argument cannot be applied to the modeling of reacting scalars because, for moderate to high reaction rates, the scale of the entire flame lies below the grid scale. Hence, the chemistry model must be capable of approximating the physical interaction between the species within each LES grid cell. One strategy for accounting for subgrid-scale (SGS) mixing is to employ an assumed form for the probability density function (PDF) of a conserved scalar within a grid volume [1]. Gao and O'Brien [2] refer to this type of PDF as a large-eddy probability density function (LEPDF) while Colucci et al. [3] refer to it as the filtered density function. Bilger [4] and Lentini [5] found that errors in assumed PDFs are greatly reduced upon integration, a common operation which is required in order to obtain, e.g., average concentrations. Frankel et al. [6] and Cook and Riley [7] demonstrated the assumed LEPDF approach to be both practical and accurate for LES with equilibrium chemistry.

To treat nonequilibrium chemistry, information in addition to the amount of SGS mixing is required. One approach is to employ a joint PDF for the SGS species mass fractions [6]. Specification of the joint LEPDF requires modeling of the subgrid-scale species covariance, a quantity that is very difficult to obtain accurately. An alternative method of accounting for non-equilibrium chemistry is to invoke the quasi-steady version of the flamelet approximation of Peters [8], Cook, Riley, Kosály, and de Bruyn Kops [9–12] have used flamelet theory, in conjunction with an assumed LEPDF, to derive a model for predicting the filtered species concentrations in LESs. The model, termed the large-eddy laminar flamelet model (LELFM), requires information about the amount and the rate of SGS mixing in the form of the subgrid-scale scalar variance and the filtered scalar dissipation rate. Those four papers show LELFM to be promising, but do not adequately address the problem of modeling the SGS mixing.

The purpose of this paper is to systematically evaluate several SGS mixing models required for mixture fraction based LES models. The models are tested *a priori* and *a posteriori* using data from high resolution direct numerical simulations and lower resolution large-eddy simulations of the classic experiment in decaying, homogeneous, isotropic, isothermal turbulence of Comte-Bellot and Corrsin [13]. Although the theory behind the mixing models is more general, this canonical flow is studied in order to identify the characteristics of the models, to eliminate questions about the accuracy of the simulation, and thus the mixing process, and because a mixing model should presumably be accurate for the simpler case if it is to be reliably accurate for more complex flows.

2 LES Models

Large-eddy simulation involves the numerical solution of the equations for momentum and scalar transport to which a filter of characteristic width Δ has been applied to remove length scales too small to be resolved on the numerical grid. The filtering operation, denoted by an overbar and defined as the convolution integral of the field with a filter kernel, results in flux terms which must be modeled. In this work, the Smagorinsky [14] model is used to relate each subgrid-scale flux to the corresponding gradient of the resolved-scale velocity component (or scalar) via a dynamically computed SGS viscosity (diffusivity). The dynamic aspect was first proposed by Germano et al. [15], with further development by, e.g., Germano [16], Lilly [17], Carati et al. [18] and Piomelli and Liu [19]. The resulting LES transport equations are:

$$\frac{\partial \overline{u}_i}{\partial t} + \frac{\partial \overline{u}_i \overline{u}_j}{\partial x_j} = -\frac{\partial \overline{p}}{\partial x_i} + 2\frac{\partial}{\partial x_j}[(\nu+\nu_T)\overline{S}_{ij}], \tag{1}$$

$$\frac{\partial \overline{\xi}}{\partial t} + \overline{u}_j \frac{\partial \overline{\xi}}{\partial x_j} = \frac{\partial}{\partial x_j}\left[(D+D_T)\frac{\partial \overline{\xi}}{\partial x_j}\right], \tag{2}$$

where $\overline{S}_{ij}$ is the resolved strain-rate tensor, ν and D are the kinematic viscosity and molecular diffusivity, and ν_T and D_T are their SGS counterparts defined in terms of the magnitude of the filtered

Contributed by the Fluids Engineering Division for publication in the JOURNAL OF FLUIDS ENGINEERING. Manuscript received by the Fluids Engineering Division September 13, 1999; revised manuscript received February 20, 2000. Associate Editor: P. E. Raad.

strain rate tensor as $\nu_T = C\Delta^2|\overline{S}|$ and $D_T = C_\xi \Delta^2 |\overline{S}|$. Both the velocity field and the scalar field, ξ, are statistically homogeneous and isotropic, so that the coefficients C and C_ξ can be considered as constant in space but as functions of time. The scalar, ξ, can be any conserved scalar, but is taken to be the mixture fraction as defined by Bilger [4], with the assumption of equal diffusivities of all species.

2.1 Subgrid-scale Chemistry Model. Our particular motivation for the current research is to develop mixing models for use with the LELFM [9–12], which we use here as a specific example of how SGS mixing models can incorporated into LES chemistry models. While the LELFM is only one approach to modeling species interactions in an LES, mixture fraction based methods in general require information about the amount of mixing at the subgrid scale if equilibrium chemistry is assumed, and information about the amount and rate of mixing for non-equilibrium analysis. For the LELFM and other mixture fraction based models, the mixing statistics required are the filtered mixture fraction, $\overline{\xi}$, the SGS scalar variance, ξ_v^2, and the filtered scalar dissipation rate, $\overline{\chi} = 2D\overline{(\partial\xi/\partial x_i)^2}$. Here, $\xi_v^2 = \overline{\xi^2} - \overline{\xi}^2$, which corresponds to the variance of the filtered probability density function as defined by Gao and O'Brien [2]; an alternative definition $\overline{(\xi - \overline{\xi})^2}$ is incorrect in general since it cannot correspond to any one point PDF [7,20]. The filtered mixture fraction is computed directly in an LES from (2). Models for ξ_v^2 and $\overline{\chi}$ are discussed in the following sections.

2.1.1 Subgrid-Scale Variance. The SGS variance can be modeled directly or it can be computed from $\overline{\xi}^2$ and $\overline{\xi^2}$, the latter of which must be modeled. Schmidt and Schumann [21] compute $\overline{\xi^2}$ by integrating its governing equation. One difficulty with this method is in developing the initial $\overline{\xi^2}$ field. Another is that it requires an additional model to account for the SGS flux of the scalar variance.

Two models have been proposed for directly modeling ξ_v^2; one relates it to the magnitude of the resolved scale gradient [22,23], the other relates it to a test scale variance [7]. The first is denoted ξ_{m1}^2 and defined $\xi_{m1}^2 \equiv \gamma\Delta^2|\nabla\overline{\xi}|^2$. The derivation starts by defining a test-scale filter of characteristic width $\hat{\Delta}$ and denoted by $\hat{(\ )}$, where $\hat{\Delta} > \Delta$, and assuming that the scalar variance below the test scale can be modeled in a manner analogous to ξ_{m1}^2. Then

$$\widehat{\overline{\xi^2}} - \hat{\overline{\xi}}^2 = \gamma\hat{\Delta}^2|\nabla\hat{\overline{\xi}}|^2 - \widehat{\gamma\Delta^2|\nabla\overline{\xi}|^2}, \tag{3}$$

and

$$\gamma = \frac{\widehat{\overline{\xi^2}} - \hat{\overline{\xi}}^2}{\hat{\Delta}^2|\nabla\hat{\overline{\xi}}|^2 - \Delta^2|\hat{\nabla}\overline{\xi}|^2}, \tag{4}$$

assuming that γ varies slowly enough in space so that it can be taken outside the test filter. Unlike the formulations for C and C_ξ, (4) does not involve averages in the homogeneous directions, so γ is a function of space.

In the second model for ξ_v^2, denoted ξ_{m2}^2, the subgrid-scale variance is estimated by assuming similarity between the subgrid-scales and the smallest resolved scales. A test filter-scale variance is defined $Z_v^2 \equiv \widehat{\overline{\xi^2}} - \hat{\overline{\xi}}^2$, which is simply the variance of $\overline{\xi}$ within subvolumes defined by the test filter width. The model assumes scale similarity between Z_v^2 and ξ_v^2, i.e.,

$$\xi_v^2 \approx \xi_{m2}^2 \equiv c_{\xi 2}(\widehat{\overline{\xi^2}} - \hat{\overline{\xi}}^2). \tag{5}$$

The quantity $c_{\xi 2}$ is computed by assuming a form for the SGS scalar energy spectrum and adding it to the resolved-scale spectrum (from the LES) to form the complete scalar energy spectrum, $E_\xi(k)$. Here k is the magnitude of the three-dimensional wave number vector. By assuming homogeneous, isotropic turbulence, Cook [24] shows that

$$c_{\xi 2} = \frac{\int_0^\infty [1 - \tilde{g}^2(k;\Delta)]E(k)dk}{\int_0^\infty [1 - \tilde{h}^2(k;\hat{\Delta})][1 - \tilde{g}^2(k;\Delta)]E(k)dk}, \tag{6}$$

where $\tilde{g}$ and $\tilde{h}$ are the Fourier transformed grid and test filters, respectively. With $c_{\xi 2}$ computed from (6), the average SGS variance from (5) will exactly equal the average SGS variance implicit in $E_\xi(k)$ if the turbulence is homogeneous and isotropic [24].

In a high Reynolds number LES, the inertial range will extend to wavenumbers which make an insignificant contribution to the SGS variance. If the grid filter is in the inertial range, it is reasonable to assume $E_\xi(k) \propto k^{-5/3}$ for all SGS k, and to ignore details of the spectrum in the dissipation range. In moderate Reynolds number flows, such as that presented in this work, the dissipation range accounts for a significant amount of the SGS variance and cannot be ignored. Instead, a form for the high wavenumber spectrum derived by Corrsin [25] and Pao [26] is used:

$$E_\xi(k) = Ak^\alpha \exp\left(-\frac{3}{2}nD\varepsilon_T^{-1/3}k^{4/3}\right). \tag{7}$$

In model ξ_{m2}^2, $\alpha = -5/3$ and $n = 0.59$, which are the values used by Pao [26]. The constant of proportionality in (7) is determined by matching $E_\xi(k)$ to the actual LES spectrum near the highest resolved wave number. The kinetic energy flux supplied by the large eddies, ε_T, can be estimated from the LES by assuming that it is equal to the energy removed from the resolved scales by the LES SGS model. Pao points out that the ε_T used for the theoretical deduction of (7) (which assumes infinite Reynolds number) will always be greater than that measured in a laboratory experiment; presumably, this is also the case for the LES of a flow with finite Reynolds number. Therefore, (7) is expected to underestimate the true SGS spectrum. While the effect that the error in E_ξ will have on ξ_{m2}^2 is not clear due to the application of the grid and test filters in (5), it is expected that $\langle\xi_{m2}^2\rangle \to \langle\xi_v^2\rangle$ as the Reynolds number increases, where $\langle\ \rangle$ denotes a spatial average.

Two additional models for ξ_v^2 are defined which improve on ξ_{m1}^2 and ξ_{m2}^2. The first, ξ_{m3}^2, is identical to ξ_{m2}^2 except that α and n are chosen so that the assumed spectrum more closely matches the spectrum of the flow being studied. This is important for moderate Reynolds number flows in which no true inertial range exists. Formally, $\xi_{m3}^2 \equiv c_{\xi 3}(\widehat{\overline{\xi^2}} - \hat{\overline{\xi}}^2)$. The second is a hybrid of models ξ_{m1}^2 and ξ_{m3}^2: $\xi_{m4}^2 \equiv c_{\xi 4}\Delta^2|\nabla\overline{\xi}|^2$. Analogous to $c_{\xi 3}$, $c_{\xi 4}$ is computed so that $\langle\xi_{m4}^2\rangle$ equals the average SGS variance computed from the assumed spectrum. Values of α and n are tailored for the flow being studied.

It is worthwhile to note that an assumed form for the three-dimensional scalar energy spectrum is utilized in this work because the scalar field in the numerical simulations is homogeneous and isotropic. The assumed spectrum technique works equally well when the scalar field is not isotropic but is homogeneous in at least one direction, so that a form for the one-dimensional energy spectrum can be assumed. For these results, see [27]. The assumed spectrum methods may also work well when the scalar field is locally isotropic on the LES grid.

2.1.2 Filtered Dissipation Rate. The filtered dissipation rate, $\overline{\chi}$, can be decomposed into three terms which represent (1) the cointeractions between the resolved scales, (2) the cointeractions between the unresolved scales, and (3) the interactions between the resolved and unresolved scales. The first of these can be computed directly from the resolved scales of an LES. Girimaji and Zhou [28] develop models for the second and third terms, and note that the backscatter (third) term must be accounted for if $\overline{\chi}$ is to be used to close the transport equation for the filtered scalar

energy. Here, two somewhat simpler classes of models are developed. In the first, denoted $\overline{\chi}_{m1}$, $\overline{\xi}$ is related to the resolved scale dissipation rate via the total diffusivity, $D+D_T$. In the second ($\overline{\chi}_{m2}$,$\overline{\chi}_{m3}$), scale similarity arguments are used to estimate $\overline{\chi}$.

To develop the first model, consider the equation for $\overline{\xi}$-energy obtained by multiplying (2) by $\overline{\xi}$ and simplifying. The resulting term for the dissipation rate of $\overline{\xi}^2$ due to molecular effects and to transfer of $\overline{\xi}$ energy to the subgrid-scales is $2(D+D_T)\times(\partial\overline{\xi}/\partial x_j)^2$. At the larger scales, $\overline{\xi^2}$ is approximately equal to $\overline{\xi}^2$, the difference between the two being due to the filtering of ξ at the smaller scales. This implies, in particular, that the transfer rate of both quantities to the subgrid scales is nearly identical. Assuming in addition that the transfer rate of ξ to the subgrid scales is equal to its dissipation rate at those scales leads to a model for $\overline{\chi}$:

$$\overline{\chi}_{m1} \equiv 2(D+D_T)\,\frac{\overline{\partial\overline{\xi}\partial\overline{\xi}}}{\partial x_i \partial x_i}. \tag{8}$$

This is similar to a term in a model for $\overline{\chi}$ proposed by Girimaji and Zhou [28].

The second model for $\overline{\chi}$ is defined as

$$\overline{\chi}_{m2} \equiv c_{\chi 2} D\,\frac{\overline{\partial\overline{\xi}\partial\overline{\xi}}}{\partial x_i \partial x_i}, \tag{9}$$

where the constant $c_{\chi 2}$ is determined by assuming a form for the high wavenumber portion of the ξ energy spectrum, e.g., (7). The derivation is similar to that of $c_{\xi 2}$. In essence, $c_{\chi 2}$ is set so that $\langle\overline{\chi}_{m2}\rangle$ is equal to the dissipation rate computed using the SGS portion of the assumed spectrum. It was argued in the previous section that the assumed SGS $E_\xi(k)$ from (7) will always underestimate the true SGS spectrum because (7) was deduced for the case of infinite Reynolds number. While the effect of the error in $E_\xi(k)$ on ξ^2_{m2} is not obvious, it is clear that underpredicting $E_\xi(k)$ at high wavenumbers will result in $\langle\overline{\chi}_{m2}\rangle<\langle\overline{\chi}\rangle$. It is expected that $\langle\overline{\chi}_{m2}\rangle\approx\langle\overline{\chi}\rangle$ for large enough Reynolds number. Analogous to ξ^2_{m2} is a third model for $\overline{\chi}$, denoted $\overline{\chi}_{m3}$, in which the coefficient $c_{\chi 2}$ is replaced by $c_{\chi 3}$ computed by assuming a form for $E_\xi(k)$ which is tailored to the flow being studied.

3 Numerical Simulations

Data from DNS are used for *a priori* testing of the LELFM and the submodels. The velocity field simulated is that of the laboratory experiment of Comte-Bellot and Corrsin [13] in which nearly isotropic, incompressible turbulence decays downstream of a grid of spacing M oriented normal to a uniform, steady flow. Statistical data were collected in the laboratory at downstream locations $x/M=42$, 98, and 171. The Reynolds number at the first station, based on the Taylor length scale and the rms velocity, is 71.6. The DNS are performed with a pseudo-spectral code using a 512^3-point periodic domain considered to be moving with the mean flow. Taylor's hypothesis is invoked to relate simulated time to laboratory coordinates. The DNS velocity field is initialized to match the laboratory kinetic energy spectrum at $x/M=42$. In the computer code, Fourier pseudo-spectral methods are used to approximate spatial derivatives, and a second-order Adams-Bashforth scheme with pressure-projection is used for time-stepping.

To test the LELFM *a posteriori*, large-eddy simulations were run on numerical grids having 64^3 and 128^3 points. In the simulations, the same pseudo-spectral code that was used for the DNS is employed, with the addition of models for the SGS fluxes, to solve (1) and (2). The LES are initialized with filtered DNS fields at $x/M=42$.

3.1 Spatial and Temporal Accuracy. The direct numerical simulations are among the largest that can be run on presently existing super-computers, and standard spatial resolution tests such as comparing results computed with different numerical grid resolutions are not possible. Nevertheless, several attributes of the simulations indicate that they are extremely accurate. First, the pseudospectral method used has the advantages that phase errors are very small, rates of convergence are very high, and the truncation error decreases faster than algebraically as the number of Fourier modes becomes large [29]. The method has been found to be twice as accurate as finite-difference schemes using the same resolution [30]. Second, spatial resolution tests typically performed for spectral simulations, including observing the evolution of the kinetic and scalar energy dissipation rate spectra and energy transfer spectra show that the largest and smallest dynamically relevant length scales are resolved on the numerical grid. Third, the simulations match the data from the highly respected wind tunnel experiments of Comte-Bellot and Corrsin [13]. The simulation results agree with the laboratory data not just for gross statistics such as average kinetic energy and integral length scale at a single downstream location but, in addition to other higher-order statistics, for the entire three-dimensional kinetic energy spectra from $x/M=42$ to $x/M=171$. For additional discussion of the simulations, see [27,31].

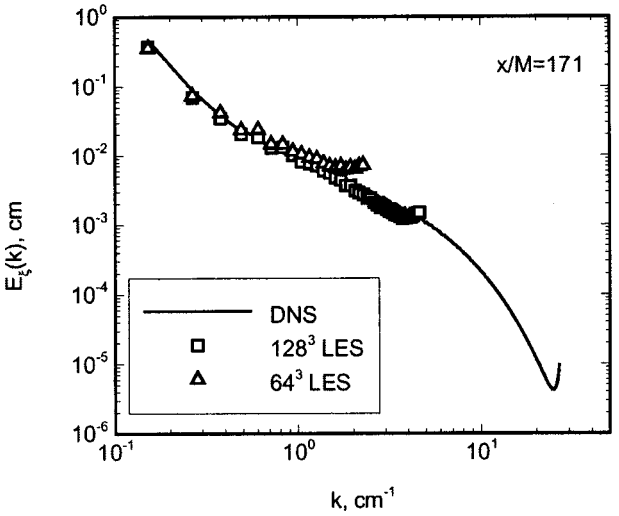

Fig. 1 Three dimensional scalar energy spectra from DNS and LES.

In LESs, the simulation results will change when the grid resolution is increased unless the closure models for the transport equations are perfect. The question becomes what grid resolution is required to accurately predict the length scales of interest. In the current simulations, it was found that about 48^3 grid points are required to accurately predict the growth rate of the integral length scale and the decay rate of the turbulence kinetic energy. These results are consistent with those of Carati et al. [18] for large-eddy simulations of the same flow. In this work, 64^3-point simulations are the lowest resolution reported, since the performances of the SGS mixing models deteriorate markedly when applied to grids coarser than this. The three dimensional scalar energy spectra at $x/M=171$ from 64^3-point and 128^3-point simulations are compared with the corresponding spectrum from the DNS in Fig. 1. There are inaccuracies in the results from both LESs near the smallest resolved scale, but the large scales and the scalar energies are accurate throughout the simulations. Additional details concerning the large eddy simulations can be found in [12,27].

The temporal accuracy of all the simulations was verified by running portions of the simulations with time step sizes differing by a factor of two and noting no measurable difference in the resulting velocity and scalar fields. Using a third order Adams-Bashforth scheme for portions of the simulations also had no effect on the results.

Table 1 Correlation coefficient between the exact filtered dissipation rate, $\overline{\chi}_e$, and related quantities

Grid	x/M	$\overline{\nabla\xi\cdot\nabla\xi}$	$\overline{\chi}_{m1}$	$\overline{\chi}_{m2}$	$\overline{\chi}_{m3}$
32^3	98	0.84	0.76	0.84	0.84
	181	0.79	0.74	0.79	0.79
64^3	98	0.83	0.79	0.83	0.83
	181	0.83	0.81	0.83	0.83

Table 3 Correlation coefficient between the SGS-variance and related quantities

Grid	x/M	$\overline{\nabla\xi\cdot\nabla\xi}$	ξ^2_{m1}	ξ^2_{m2}	ξ^2_{m3}	ξ^2_{m4}
32^3	98	0.93	0.79	0.87	0.87	0.93
	181	0.91	0.74	0.82	0.82	0.91
64^3	98	0.92	0.78	0.84	0.84	0.92
	181	0.91	0.76	0.82	0.82	0.91

4 Results

4.1 A Priori Evaluation of the Models for $\overline{\chi}$. The models for $\overline{\chi}$ are evaluated *a priori* by filtering the 512^3 DNS data onto coarser grids to simulate LES data. The modeled quantities are computed from these filtered fields and compared with the exact filtered dissipation rate, $\overline{\chi}_e$, determined by filtering χ from the DNS. Two filter widths are used, which result in simulated LES fields having 32^3 and 64^3 points.

A good model for $\overline{\chi}$ will be well correlated with $\overline{\chi}_e$ and also will have approximately the same volume average. The correlation between $\overline{\chi}_e$ and related quantities is given in Table 1, and the corresponding mean values, as fractions of $\langle\overline{\chi}_e\rangle$, in Table 2. The factor $\overline{\nabla\xi\cdot\nabla\xi}$ is common to $\overline{\chi}_{m1}$, $\overline{\chi}_{m2}$, and $\overline{\chi}_{m3}$, and there is good correlation between it and the exact filtered dissipation rate. This fact is encouraging because it implies that a model for $\overline{\chi}$ might be based upon $\overline{\nabla\xi\cdot\nabla\xi}$, provided that a method can be found to adjust the mean value of the model appropriately.

In model $\overline{\chi}_{m1}$, the SGS diffusivity, D_T, is used to scale $\overline{\nabla\xi\cdot\nabla\xi}$, and, since D_T is neither constant in space nor well correlated with $\overline{\chi}_e$, this approach adversely affects the correlation between the exact and modeled dissipation rates, but not by a great amount. Of greater concern is that $\langle\overline{\chi}_{m1}\rangle$ is about a quarter of $\langle\overline{\chi}_e\rangle$ in the 32^3 domain and about half $\langle\overline{\chi}_e\rangle$ in the 64^3 domain. In the model, it is assumed that the sum of the molecular and SGS dissipation rates of ξ-energy from the resolved scales, $\langle\chi_{gs}\rangle$, is approximately equal to the dissipation rate from all scales, $\langle\overline{\chi}_e\rangle$. The ratio $\langle\chi_{gs}\rangle/\langle\overline{\chi}_e\rangle$ is only about 0.3 to 0.4 in the 64^3 LES, and an LES grid larger than 128^3 would be required to make the ratio 0.8. The scalar fields depend strongly on the initial conditions, so that it is probable that $\langle\chi_{gs}\rangle$ is a better approximation of $\langle\overline{\chi}_e\rangle$ in some configurations than others. Since the velocity field is driving the transfer of scalar energy from large to small scales, however, it is useful to examine the corresponding relationship for the velocity field; in the 64^3 LES, only about 70% of the kinetic energy dissipation is due to transfer and dissipation from the large scales, and the fraction drops to about 50% for the 32^3 fields. The conclusion is that $\langle\overline{\chi}_{m1}\rangle$ will underestimate $\langle\overline{\chi}_e\rangle$ by 30–75%, depending on the resolution of the LES and the flow configuration.

In model $\overline{\chi}_{m2}$, $\overline{\nabla\xi\cdot\nabla\xi}$ is scaled by a coefficient which has a value such that $\langle\overline{\chi}_{m2}\rangle$ will equal the average dissipation rate computed from a composite dissipation rate spectrum made up of the known resolved scale spectrum and an assumed form for the unresolved scales. The coefficients in the assumed spectrum (7) are those given by Pao [26]. In the present flow, the slope of $E_\xi(\kappa)$ is flatter than $-5/3$ at the highest resolved wave number, especially in the 32^3 LES, so the peak of the assumed $D_\xi(\kappa)$ is lower than the true peak in the dissipation rate spectrum and $\langle\overline{\chi}_{m2}\rangle$ underpredicts $\langle\overline{\chi}_e\rangle$. In model $\overline{\chi}_{m3}$, the coefficients of (7) are adjusted to $\alpha=-1$ and $n=1.2$. From Table 2, it is clear that the model accurately predicts the filtered dissipation rate, provided that the shape of the ξ-energy spectrum is reasonably well known. The strength of the model is that it is based on the transfer of kinetic energy out of the resolved scales, which the LES predicts very accurately. If the LES cannot accurately predict the resolved-scale dissipation rate, the evolution of the velocity and scalar fields will be incorrect and the modeling of $\overline{\chi}$ is moot.

4.2 A Priori Evaluation of the Models for ξ^2_v. Like the models for $\overline{\chi}$, the approximations for ξ^2_v are based on quantities that can be computed locally in the LES and scaled so that the mean SGS variance is approximately correct. In model ξ^2_{m1}, $\overline{\nabla\xi\cdot\nabla\xi}$, is multiplied by a dynamically computed coefficient, γ, which is a function of space and time. From Table 3, it is clear that $\overline{\nabla\xi\cdot\nabla\xi}$ is a good quantity on which to base a model because it is highly correlated with ξ^2_e over the full range of x/M and LES resolution. In the computation of γ, however, it is assumed that the SGS-variance can be predicted from a test-scale variance, which is a poor assumption for the present flow. Even if the flow were such that γ were approximately the correct factor with which to relate $\overline{\nabla\xi\cdot\nabla\xi}$, with ξ^2_e, it is poorly correlated with ξ^2_e and significantly degrades the correlation between ξ^2_{m1} and ξ^2_e.

In models ξ^2_{m2} and ξ^2_{m3}, it is again postulated that the SGS variance can be related to a test-scale variance, but this time the relationship is through the correlation and not the mean. The distinction between ξ^2_{m2} and ξ^2_{m3} is the same as that between $\overline{\chi}_{m2}$ and $\overline{\chi}_{m3}$, namely that ξ^2_{m2} is based on a generic assumed spectrum and ξ^2_{m3} is based on a spectrum tailored for the current flow configuration. Both $\langle\xi^2_{m2}\rangle$ and $\langle\xi^2_{m3}\rangle$ are excellent estimates of $\langle\xi^2_e\rangle$ (Table 4), but the correlation is only moderately good in view of the excellent correlation between ξ^2_e and $\overline{\nabla\xi\cdot\nabla\xi}$. In model ξ^2_{m4}, the concept of relating the SGS variance to a test-scale variance is discarded and $\overline{\nabla\xi\cdot\nabla\xi}$ is scaled the same way $(\widehat{\xi^2}-\hat{\xi}^2)$ is scaled in model ξ^2_{m3}. The result is a model that almost exactly matches $\langle\xi^2_e\rangle$ with excellent correlation.

4.3 A Posteriori Tests. It is the accuracies of $\overline{\chi}$ and ξ^2_v when computed from an LES which are of prime interest, although the models cannot be validated on a point-wise basis as they can be when applied to filtered DNS data. In the current simulations, the scalar dissipation rate from the smallest resolved-scales is slightly too high, and the resolved-scale scalar variance is correspondingly low (Fig. 1). This causes $\overline{\chi}_{m1}$ to perform better than expected from the *a priori* tests, but still significantly worse than $\overline{\chi}_{m3}$ at most downstream locations, as shown in Fig. 2(*a*). *A*

Table 2 Mean values of various quantities as fractions of $\langle\overline{\chi}_e\rangle$

Grid	x/M	$\overline{\nabla\xi\cdot\nabla\xi}$	$\overline{\chi}_{m1}$	$\overline{\chi}_{m2}$	$\overline{\chi}_{m3}$
32^3	98	0.026	0.19	0.55	0.89
	181	0.049	0.24	0.74	0.96
64^3	98	0.067	0.34	0.65	0.89
	181	0.13	0.45	0.83	0.96

Table 4 Mean values of various quantities as fractions of $\langle\xi^2_e\rangle$

Grid	x/M	ξ^2_{m1}	ξ^2_{m2}	ξ^2_{m3}	ξ^2_{m4}
32^3	98	0.57	0.93	0.98	0.98
	181	0.62	0.94	0.97	0.97
64^3	98	0.71	0.98	0.99	0.99
	181	0.75	0.99	0.99	0.99

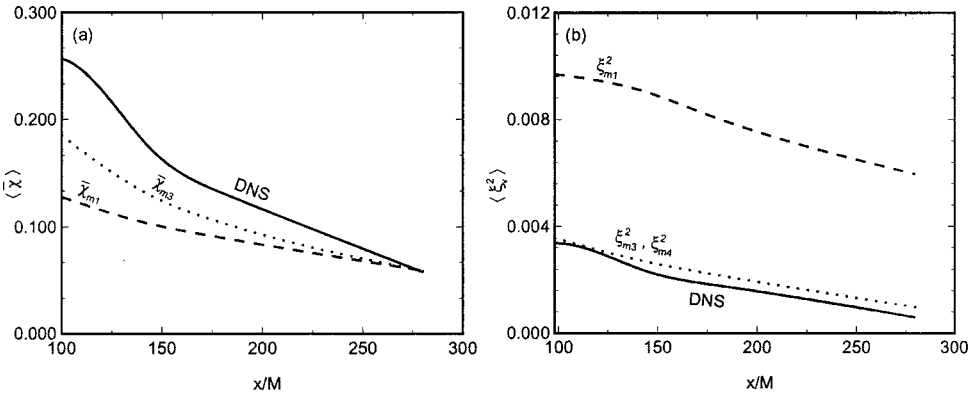

Fig. 2 LES predictions for $\bar{\chi}$ (*a*) and ξ_v^2 (*b*), compared to DNS values, from 64^3 LES

priori tests of ξ_{m1}^2 show that it underpredicts ξ_e^2, whereas it significantly overpredicts the exact value in an actual LES (Fig. 2*b*). Both ξ_{m2}^2 and ξ_{m3}^2 are very good, but not nearly perfect as suggested by the tests with DNS data.

When the resolution of the LES is increased to 128^3-points (not shown), the models that depend on an assumed spectrum improve dramatically [27]. This is in part due to the fact that more of the spectrum is computed directly in a higher resolution LES, and so less must be estimated. The principal problem, however, in estimating the spectra for the current (moderate Reynolds number) flow is that there is no inertial range, which makes the parameter α in (7) difficult to estimate. The spectra for flows with higher Reynolds number may be easier to estimate from 64^3-point LES data.

5 Conclusions

Information about mixing at scales smaller than those resolved on an LES numerical grid is needed if mixture fraction based models are to be used for predicting species concentrations in LESs of non-premixed, turbulent reacting flows. For example, the large-eddy laminar flamelet model requires submodels for the SGS scalar variance and the filtered scalar dissipation rate to provide information about SGS mixing. Several formulations for each submodel are presented and tested using filtered DNS data and LES results. Predictions from the models that depend on an assumed form for the scalar energy spectrum are very good for the flow considered, and are better than those from models that rely on other assumptions. Additionally, the spectrum-based models perform consistently when tested *a priori* and *a posteriori* at several different LES resolutions, which encourages the thought that the models are robust. In contrast, several of the other models tested behave differently in *a priori* and *a posteriori* tests, and the accuracy of the model predictions varies widely as the scalar field develops with downstream distance. Since the spectrum-based models are applicable to flows for which a form for the one-dimensional scalar energy can be estimated [12], these models show promise for a variety of flow configurations.

Acknowledgments

This work is supported by the National Science Foundation (grant no. CTS9810103) and the Air Force Office of Scientific Research (grant no. F49620-97-1-0092), and by grants of high performance computing (HPC) time from the Arctic Region Supercomputing Center and the Pittsburgh Supercomputing Center.

References

[1] Givi, P., 1989, ''Model free simulations of turbulent reactive flows,'' Prog. Energy Combust. Sci., **15**, pp. 1–107.
[2] Gao, F., and O'Brien, E. E., 1993, ''A large-eddy simulation scheme for turbulent reacting flows,'' Phys. Fluids A, **5**, pp. 1282–1284.
[3] Colucci, P. J., Jaberi, F. A., Givi, P., and Pope, S. B., 1998, ''Filtered density function for large eddy simulation of turbulent reacting flows,'' Phys. Fluids, **10**, No. 2, pp. 499–515.
[4] Bilger, R. W., 1980, ''Turbulent flows with nonpremixed reactants,'' P. A. Libby and F. A. Williams, editors, *Topics in Applied Physics Number 44: Turbulent Reacting Flows*, chapter 3, Springer, New York, pp. 65–113.
[5] Lentini, D., 1994, ''Assessment of the stretched laminar flamelet approach for non-premixed turbulent combustion,'' Combust. Sci. Technol., **100**, pp. 95–122.
[6] Frankel, S. H., Adumitroaie, V. Madnia, C. K., and Givi, P. 1993, ''Large-eddy simulation of turbulent reacting flows by assumed PDF methods.'' *Engineering Applications of Large Eddy Simulations*, New York, ASME, pp 81–101.
[7] Cook, A. W. and Riley, J. J., 1994, ''A subgrid model for equilibrium chemistry in turbulent flows.'' Phys. Fluids, **6**, No. 8, pp. 2868–2870.
[8] Peters, N., 1984, ''Laminar diffusion flamelet models in non-premixed turbulent combustion,'' Prog. Energy Combust. Sci., **10**, pp. 319–339.
[9] Cook, A. W., Riley, J. J., and Kosály, G., 1997, ''A laminar flamelet approach to subgrid-scale chemistry in turbulent flows,'' Combust. Flame, **109**, pp. 332–341.
[10] Cook, A. W., and Riley, J. J., 1997, ''Subgrid-scale modeling for turbulent, reacting flows,'' Combust. Flame, **112**, pp. 593–606.
[11] de Bruyn Kops, S. M., Riley, J. J., Kosály, G., and Cook, A. W., 1998, ''Investigation of modeling for non-premixed turbulent combustion,'' Flow, Turbul. Combust., **60**, No. 1, pp. 105–122.
[12] de Bruyn Kops, S. M., and Riley, J. J., ''Large-eddy simulation of non-premixed reacting flows with realistic chemistry,'' Comput. Math. Appl., to appear.
[13] Comte-Bellot, G. and Corrsin, S., 1971, ''Simple Eulerian time correlation of full and narrow-band velocity signals in grid-generated, 'isotropic' turbulence,'' J. Fluid Mech., **48**, pp. 273–337.
[14] Smagorinsky, J., 1963, ''General circulation experiments with the primitive equations. I. The basic experiment,'' Mon. Weather Rev., **91**, pp. 99–164.
[15] Germano, M., Piomelli, U., Moin, P., and Cabot, W. H., 1991, ''A dynamic subgrid-scale eddy viscosity model,'' Phys. Fluids A, **3**, pp. 1760–1765.
[16] Germano, M., 1992, ''Turbulence: the filtering approach,'' J. Fluid Mech., **238**, pp. 325–336.
[17] Lilly, D. K., 1992, ''A proposed modification of the Germano subgrid-scale closure method,'' Phys. Fluids A, **4**, pp. 633–635.
[18] Carati, D., Ghosal, S., and Moin, P., 1995, ''On the representation of backscatter in dynamic localization models,'' Phys. Fluids, **7**, No. 3, pp. 606–616.
[19] Piomelli, U., and Liu, J., 1995, ''Large-eddy simulation of rotating channel flows using a localized dynamic model,'' Phys. Fluids A, **7**, pp. 839–848.
[20] Jiménez, C. F. Ducros, and B. Cuenot, 2000, ''Subgrid scale variance and dissipation of a scalar field in large eddy simulation combustion models,'' 8th European Turbulence Conference, Barcelona, Spain.
[21] Schmidt, H., and Schumann, U., 1999, ''Coherent structure of the convective boundary layer derived from large-eddy simulations,'' J. Fluid Mech., **200**, pp. 511–562.
[22] Yoshizawa, A., 1986, ''Statistical theory for compressible turbulent shear flows, with the application to subgrid modeling,'' Phys. Fluids A, **29**, pp. 2152–2164.
[23] Mathey, F., and J. P. Chollet, 1996, ''Sub-grid model of scalar mixing for large eddy simulations of turbulent flows,'' The Second ERCOFTAC Workshop on Direct and Large Eddy Simulations, Grenoble, France.
[24] Cook, A. W., 1997, ''Determination of the constant coefficient in scale similarity models of turbulence,'' Phys. Fluids, **9**, No. 5, pp. 1485–1487.
[25] Corrsin, S., 1964, ''Further generalizations of Onsager's cascade model for turbulent spectra,'' Phys. Fluids, **7**, pp. 1156.
[26] Pao, Yih Ho, 1965, ''Structure of turbulent velocity and scalar fields at large wavenumbers,'' Phys. Fluids, **8**, No. 6, pp. 1063–1075.

[27] de Bruyn Kops, S. M., 1999, ''*Numerical Simulation of Non-premixed Turbulent Combustion*'' PhD thesis, University of Washington.
[28] Girimaji, S. S., and Zhou, Y., 1996, ''Analysis and modeling of subgrid scalar mixing using numerical data,'' Phys. Fluids A, **8**, No. 5, pp. 1224–1236.
[29] Gottlieb, D., and S. A. Orszag, 1977, ''*Numerical Analysis of Spectral Methods: Theory and Applications*,'' Vol. 26, *NSF-CBMS, Regional Conference Series in Applied Mathematics*. Society of Industrial and Applied Mathematics, Philadelphia.
[30] Peyret, P., and T. D. Taylor, 1993, *Computational Methods for Fluid Flows*, Springer, New York.
[31] de Bruyn Kops, S. M., Riley, J. J., 1998, ''Direct numerical simulation of laboratory experiments in isotropic turbulence,'' Phys. Fluids, **10**, No. 9, pp. 2125–2127.